Int. J. Heat Mass Transfer. Vol. 35, No. 10, pp. 2579–2592, 1992
Printed in Great Britain

0017–9310/92 $5.00 + 0.00
Pergamon Press Ltd

Finite difference solution for transient radiative cooling of a conducting semitransparent square region

R. SIEGEL and F. B. MOLLS
National Aeronautics and Space Administration, Lewis Research Center, Cleveland, OH 44135, U.S.A.

(*Received* 4 *January* 1991 *and in final form* 20 *September* 1991)

Abstract—Transient solutions were obtained for a square region of heat conducting semitransparent material cooling by thermal radiation. The region is in a vacuum environment, so energy is dissipated only by radiation from within the medium leaving through its boundaries. The effect of heat conduction during the transient is to partially equalize the internal temperature distribution. As the optical thickness of the region is increased, the temperature gradients increase near the boundaries and corners, unless heat conduction is large. The solution procedure must provide accurate temperature distributions in these regions to prevent error in the calculated radiation losses. Two-dimensional numerical Gaussian integration is used to obtain the local radiative source term. A finite difference procedure with variable space and time increments is used to solve the transient energy equation. Variable spacing was used to concentrate grid points in regions with large temperature gradients.

INTRODUCTION

TRANSIENT thermal processes in semitransparent materials arise in applications using high temperature ceramic coatings and components, in processes for crystal growth by solidification in an outer space environment, and in observation windows in high temperature devices. Transient solutions are in the literature for various one-dimensional situations such as single and multiple semitransparent plane layers, and spheres. For multidimensional geometries, however, very little information exists for transient radiative processes, especially where heat conduction is included. Results are obtained here for a square region, although the basic analysis is carried out more generally for a rectangle.

In a semitransparent material where radiative transport acts simultaneously with heat conduction, the radiation fluxes depend strongly on the temperature level. Hence, during a transient calculation, accurate temperature distributions must be obtained at each time step or the error in the radiation terms will cause the results to become considerably in error as time advances.

For some types of thermal boundary conditions, approximate analytical methods, such as those developed from radiative diffusion concepts, do not yield accurate transient solutions as they cannot deal with the boundary conditions with sufficient accuracy. Although the diffusion approximation is valid in the central portion of an optically thick region, it does not apply near a boundary, and additional approximations are needed to deal with the boundary conditions. The extent of the error incurred by using the approximate boundary conditions is difficult to assess for situations that have not been examined previously in detail, such as transient solutions of the type treated here. In the present case, because the semitransparent region is cooling in a vacuum environment at a low temperature, the unknown boundary temperatures depend on both time and position.

The solution requires two numerical operations. One is integrating the radiation contribution arising from the temperature distribution surrounding each location to obtain the local transient radiative source distribution within the medium. The second is the transient solution of the energy equation using this source distribution. A Gaussian integration method is used here to evaluate the source function distribution. A finite difference procedure with variable grid and time increment sizes is used for solving the energy equation. This approach demonstrates that numerical procedures can be applied directly to the exact energy equation and boundary conditions, to yield accurate transient cooling solutions for combined radiation and conduction when the boundary temperature distribution is unknown and varies with time.

For plane layers, many steady-state solutions have been obtained as reviewed in textbooks such as ref. [1]. Although transient studies for plane layer geometries are much fewer in number, a variety of situations has been analyzed for single and multiple layers [2–10]. In the early 1980s solutions involving radiative transfer in absorbing–emitting media with nonuniform temperature distributions advanced considerably from one-dimensional to two- and some three-dimensional situations. Numerical solutions of these more difficult multidimensional cases become feasible as larger and faster computers become avail-

NOMENCLATURE

A_R	aspect ratio of rectangular region, d/b
a	absorption coefficient of layer [m^{-1}]
B_0	optical length of short side of rectangle, ab
b	length of short side of rectangle [m]
c_p	specific heat of radiating medium [$J\,kg^{-1}\,K^{-1}$]
d	length of long side of rectangle [m]
I, J	number of grid points in X and Y directions
k	thermal conductivity of radiating medium [$W\,m^{-1}\,K^{-1}$]
N	conduction–radiation parameter, $k/4\sigma T_i^3 b$
n	normal direction
Q	heat loss from entire perimeter for a unit of axial length z [$W\,m^{-1}$]
q_l, q_s	local heat fluxes leaving long and short sides [$W\,m^{-2}$]
R	separation distance in X–Y plane
$\tilde{R}$	abbreviation for radiation terms in energy equation
S_n	function defined in equation (2)
$S_{i,j}$	terms in matrix equation (A1)
T	absolute temperature [K]
T_e	temperature of surrounding environment [K]
T_i	initial temperature of radiating region [K]
T_m	integrated mean temperature [K]
t	dimensionless temperature, T/T_i
x, y, z	rectangular coordinates [m]; $X = x/b$, $Y = y/b$, $Z = z/b$.

Greek symbols

Δ	increment of length, temperature, or time
$\Delta X, \Delta Y$	grid spacings in X and Y directions
$\Delta\varphi$	intermediate value in equation (18b)
ε_m	transient emittance of region based on instantaneous values of Q and T_m
ε_{ut}	emittance for region at uniform temperature
θ	time [s]; angle in cylindrical coordinates [rad]
ρ	density of radiating medium [$kg\,m^{-3}$]
σ	Stefan–Boltzmann constant [$W\,m^{-2}\,K^{-4}$]
τ	dimensionless time, $(4\sigma T_i^3/\rho c_p b)\theta$.

Subscripts

i	initial condition; the ith X location
j	the jth Y location
m	integrated mean value over region; based on mean value
n	at the nth time increment
ut	uniform temperature condition.

able. A transient solution requires more computer time than a steady solution, since the multidimensional radiative source distribution must be evaluated at each time step. The references that follow are almost all for steady conditions. Very little has been done on multidimensional transient problems, especially when heat conduction is included.

Steady-state numerical solutions have been carried out in the literature by a number of techniques, such as using discrete ordinates [11, 12] and finite elements [13, 14]. Various expansion and numerical methods have been used in refs. [15–19]. A few transient solutions for rectangular geometries without heat conduction are in refs. [20, 21]. The present analysis used a finite difference method with implicit forward time integration, and two-dimensional Gaussian integration to evaluate the local radiative source term.

A common boundary condition is to specify surface temperatures. In the present situation the radiating region is cooling by exposure to a cold environment, and the surface temperature distribution is an unknown function of time. The environment is a vacuum, such as in outer space, and hence there is no means to remove energy from the surfaces of the region by convection or conduction. The region is semitransparent so radiant energy from within the region passes out through its boundaries. This is volume emission so there is no radiation emitted from the surface itself. Energy can be conducted to the surface, but cannot be radiated exactly from the surface since the surface has no volume. The boundary condition for the temperature distribution is that the local temperature gradient normal to each surface is zero. Heat conduction redistributes energy within the region, but energy is lost only by radiation.

For some conditions, such as for an optically thick region, the transient temperature distributions are quite curved near the boundaries. If the temperatures near the boundaries and corners are inaccurate, the radiative loss can be significantly in error. For an accurate transient solution, the zero temperature gradient boundary condition that applies for the present external conditions must be accurately achieved by the numerical procedure. Otherwise the solution will behave as if there is an additional energy loss or gain at the boundary and this leads to an accumulative error in the overall heat balance during the transient cooling calculations. To be able to obtain accurate temperature distributions near the boundaries for conditions of transient radiative loss, a finite differ-

ence procedure was used with a variable increment size to concentrate grid points in the near boundary regions.

The temperature distribution of the rectangular region is initially uniform; hence, its initial emittance is for that condition, which was analyzed analytically in ref. [22]. At the onset of transient cooling, the boundary regions cool rapidly. Unless the entire region is optically thin, this cooling reduces the overall emittance of the region since much of the radiation loss is originating from the portion adjacent to the boundaries which are at a lower temperature than is characteristic of the region interior. For an initial time period, the emittance continues to decrease with time. Then the radiation contribution to the energy exchange becomes smaller because the temperature level has decreased. The magnitude of conduction relative to radiation increases; this tends to make the temperature distribution more uniform as the transient proceeds further. The region emittance then increases toward its initial value which was for a uniform temperature region.

The variation of emittance throughout the transient depends on the optical thickness of the region, and on the initial conduction–radiation parameter which contains the thermal conductivity. For certain conditions, such as an optically thin medium, the temperature distributions tend to be rather uniform throughout the entire transient. In this instance the use of the emittance corresponding to a uniform temperature provides a very good approximation throughout the transient solution. The results will show the ranges of parameters for which this is a good approximation, thus providing a simple prediction method for the overall behavior.

ANALYSIS

Energy equation and boundary conditions for transient cooling

A rectangular region, as shown in Fig. 1(a), has side lengths b and d. It is long in the z direction so the thermal behavior is two-dimensional. The region consists of a gray emitting, absorbing, and nonscattering medium that is heat conducting. Initially the region is at uniform temperature T_i. It is then placed in much cooler surroundings at T_e so that energy is lost by radiation. The surroundings are a vacuum so that radiation emerging from within the region is the only means of energy loss. The surrounding temperature is low enough, $T_e \ll T(x, y, \theta)$, so that radiation from the surroundings to the region can be neglected. The rectangular region conducts heat internally, but because of the vacuum surroundings, there is no mechanism by which heat can be conducted or convected away from the boundaries. Hence, the normal derivative of temperature is zero along the entire boundary.

The transient energy equation has the dimensionless form [17, 18, 20]

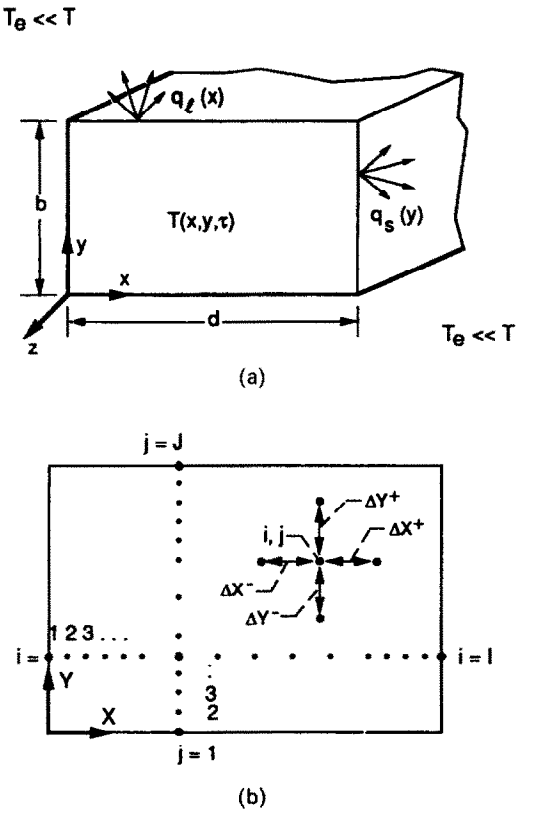

FIG. 1. Two-dimensional emitting, absorbing, and heat conducting rectangular medium. (a) Geometry and coordinate system. (b) Nomenclature for nonuniform grid.

$$\frac{\partial t}{\partial \tau} = N\left(\frac{\partial^2 t}{\partial X^2} + \frac{\partial^2 t}{\partial Y^2}\right) - B_0\left[t^4(X, Y, \tau) - \frac{B_0}{4}\int_{X'=0}^{A_R}\int_{Y'=0}^{1} t^4(X', Y', \tau)\frac{S_1(B_0 R)}{R}\,dX'\,dY'\right], \tag{1}$$

where

$$R = R(X, Y, X', Y') = [(X'-X)^2 + (Y'-Y)^2]^{1/2}.$$

Equation (1) expresses that the local change of internal energy is the result of the local net heat conduction, local radiant emission, and the gain of energy by radiation from the surrounding medium. S_1 is one of a class of S_n functions examined in ref. [23] that arise in two-dimensional radiative transfer

$$S_n(\xi) = \frac{2}{\pi}\int_0^{\pi/2} e^{-\xi/\cos\beta}\cos^{n-1}\beta\,d\beta. \tag{2}$$

As discussed later, a finite difference procedure with variable increment sizes in space and time is used to obtain the transient temperature distributions $t(X, Y, \tau)$. The initial condition for the region is $t(X, Y, 0) = 1$. Radiation passes out from within the volume, but does not originate from the surface itself (which has no volume). Consequently for all τ, the boundary conditions for a vacuum environment are,

$$\partial t/\partial X = 0 \text{ for } X = 0, A_R, \quad 0 < Y < 1,$$

and

$$\partial t/\partial Y = 0 \text{ for } Y = 0, 1, \quad 0 < X < A_R.$$

Local heat fluxes and total energy leaving boundary

The local heat flux leaving the boundary at any time is obtained by integrating over the volume the energy that arrives at a position on the boundary from each volume element. This was done in refs. [15, 20] and gave the local fluxes leaving the long and short sides in Fig. 1 as

$$\frac{q_l(X,\tau)}{\sigma T_i^4} = B_0 \int_{X'=0}^{A_R} \int_{Y'=0}^{1} t^4(X', Y', \tau) \times (1-Y') \frac{S_2(B_0 R_1)}{R_1^2} \, dY' \, dX' \quad (3a)$$

$$\frac{q_s(Y,\tau)}{\sigma T_i^4} = B_0 \int_{X'=0}^{A_R} \int_{Y'=0}^{1} t^4(X', Y', \tau) \times (A_R - X') \frac{S_2(B_0 R_2)}{R_2^2} \, dY' \, dX' \quad (3b)$$

where

$$R_1^2 = (X-X')^2 + (1-Y')^2,$$

$$R_2^2 = (A_R - X')^2 + (Y-Y')^2.$$

The instantaneous rate of energy loss from the entire boundary per unit length in the z direction is found by integrating the local fluxes over the four sides to yield

$$Q(\theta) = 2\left[\int_0^d q_l(x,\theta)\,dx + \int_0^b q_s(y,\theta)\,dy\right].$$

This has the dimensionless form

$$\frac{Q(\tau)}{2(b+d)\sigma T_i^4} = \varepsilon_i(\tau) = \frac{1}{1+A_R}\left[\int_0^{A_R} q_l(X,\tau)\,dX + \int_0^1 q_s(Y,\tau)\,dY\right]. \quad (4)$$

The $\varepsilon_i(\tau)$ is the transient overall emittance for the entire region, based on the instantaneous total energy loss and the *initial* temperature.

Local and mean emittance relations

At any time during transient cooling, the mean temperature is obtained from $T(x, y, \theta)$ by using,

$$T_m(\theta) = \frac{1}{bd}\int_{x=0}^{d}\int_{y=0}^{b} T(x,y,\theta)\,dx\,dy,$$

which gives the dimensionless form

$$\frac{T_m(\theta)}{T_i} = t_m(\tau) = \frac{1}{A_R}\int_{X=0}^{A_R}\int_{Y=0}^{1} t(X,Y,\tau)\,dX\,dY. \quad (5)$$

The instantaneous emittance $\varepsilon_m(\theta)$ for the overall heat loss, based on the *instantaneous mean* temperature, is obtained from the heat balance, $Q(\theta) = 2(b+d)\varepsilon_m(\theta)\sigma T_m^4(\theta)$. In dimensionless form, this gives

$$\varepsilon_m(\tau) = \varepsilon_i(\tau)/t_m^4(\tau). \quad (6)$$

As a check on the numerical work, $\varepsilon_m(\theta)$ was also obtained from the heat balance,

$$2(b+d)\varepsilon_m(\theta)\sigma T_m^4(\theta) = -\rho c_p bd \, dT_m(\theta)/d\theta,$$

that has the dimensionless form

$$\varepsilon_m(\tau) = -\frac{2A_R}{1+A_R}\frac{1}{t_m^4}\frac{dt_m}{d\tau}. \quad (7)$$

Since the time increments are small enough that $\varepsilon_m(\tau)$ changes only a small amount for each $\Delta\tau$, equation (7) can be integrated analytically over a small interval from τ to $\tau+\Delta\tau$ to yield

$$\varepsilon_m(\tau \text{ to } \tau+\Delta\tau) = \frac{2A_R}{1+A_R}\frac{1}{3\Delta\tau}\left[\frac{1}{t_m^3(\tau+\Delta\tau)} - \frac{1}{t_m^3(\tau)}\right]. \quad (8)$$

This provides another equality to check the consistency of the results from the numerical solution.

Relations for region at spatially uniform temperature

For comparison, transient solution results are obtained for a rectangular region that always has a spatially uniform temperature. For this situation, the emittance is a constant for each optical dimension B_0. It is called ε_{ut} and is evaluated at the beginning of each transient solution where the first set of boundary heat flux integrations is for an initially uniform temperature distribution. The ε_{ut} is also obtained in ref. [22] by another method. By integrating equation (7) with $\varepsilon_m = \varepsilon_{ut}$,

$$t_{m,ut}(\tau) = \left(1 + \frac{3}{2}\frac{1+A_R}{A_R}\varepsilon_{ut}\tau\right)^{-1/3}. \quad (9)$$

Then from $Q_{ut}(\theta) = 2(b+d)\varepsilon_{ut}\sigma T_{m,ut}^4(\theta)$, the instantaneous overall heat loss is expressed in terms of ε_{ut} and τ as

$$\frac{Q_{ut}(\tau)}{2(b+d)\sigma T_i^4} = \varepsilon_{ut}\left(1 + \frac{3}{2}\frac{1+A_R}{A_R}\varepsilon_{ut}\tau\right)^{-4/3}. \quad (10)$$

It is evident from equations (9) and (10) that if ε_{ut} is known, it is very easy to compute the transient mean temperature and overall heat loss for a region that always has a spatially uniform temperature. The results for transient cooling of the actual region that has a nonuniform temperature distribution can be conveniently presented as a ratio relative to the uniform temperature results. The mean temperature $t_m(\tau)$ for the actual transient is given relative to that for a region at spatially uniform and time varying temperature by

$$\frac{t_m(\tau)}{t_{m,ut}(\tau,\varepsilon_{ut})} = t_m(\tau)\left(1 + \frac{3}{2}\frac{1+A_R}{A_R}\varepsilon_{ut}\tau\right)^{1/3}. \quad (11)$$

Similarly the instantaneous overall heat loss $Q(\tau)$ relative to that for a region always at spatially uniform temperature is given by

$$\frac{Q(\tau)}{Q_{ut}(\tau,\varepsilon_{ut})}=\frac{\varepsilon_m(\tau)}{\varepsilon_{ut}}t_m^4(\tau)\left(1+\frac{3}{2}\frac{1+A_R}{A_R}\varepsilon_{ut}\tau\right)^{4/3}. \quad (12)$$

Procedure for numerical solution

To shorten the notation while developing the solution method for equation (1), the radiation terms on the right-hand side are called $\tilde{R}$. The equation then has the form

$$\frac{\partial t}{\partial\tau}=N\left(\frac{\partial^2 t}{\partial X^2}+\frac{\partial^2 t}{\partial Y^2}\right)-\tilde{R}(t). \quad (13)$$

By using the trapezoidal rule to integrate over a small time interval, the local temporal change in t is expressed in terms of $\partial t/\partial\tau$ at successive times by

$$\Delta t=t_{n+1}-t_n=\int_\tau^{\tau+\Delta\tau}\frac{\partial t}{\partial\tau}\,d\tau\approx\frac{\Delta\tau}{2}\left[\left(\frac{\partial t}{\partial\tau}\right)_{n+1}+\left(\frac{\partial t}{\partial\tau}\right)_n\right]. \quad (14)$$

The value of $\tilde{R}_{n+1}$ needed for obtaining $(\partial t/\partial\tau)_{n+1}$ in equation (13) is obtained in terms of $\tilde{R}_n$ by the expansion

$$\tilde{R}_{n+1}=\tilde{R}_n+\left(\frac{\partial\tilde{R}}{\partial t}\right)_n(t_{n+1}-t_n). \quad (15)$$

The second derivatives in equation (13) can be written at $\tau+\Delta\tau$ as (ξ is either X or Y),

$$\left(\frac{\partial^2 t}{\partial\xi^2}\right)_{n+1}=\frac{\partial^2(t_{n+1}-t_n)}{\partial\xi^2}+\frac{\partial^2 t_n}{\partial\xi^2}=\frac{\partial^2\Delta t_n}{\partial\xi^2}+\frac{\partial^2 t_n}{\partial\xi^2}. \quad (16)$$

Substituting equation (13) into (14) and then using equations (15) and (16), the equation to be solved for Δt becomes

$$\left[1+\frac{\Delta\tau}{2}\left(\frac{\partial\tilde{R}}{\partial t}\right)_n-\frac{\Delta\tau}{2}N\left(\frac{\partial^2}{\partial X^2}+\frac{\partial^2}{\partial Y^2}\right)\right]\Delta t=\Delta\tau\left[N\left(\frac{\partial^2 t}{\partial X^2}+\frac{\partial^2 t}{\partial Y^2}\right)_n-\tilde{R}_n\right]. \quad (17)$$

The alternating direction implicit method (ADI) will be used. A general description is given in ref. [24]; the method used here from ref. [25] differs somewhat. The second derivative operator on Δt is split into each of the coordinate directions, and equation (17) is approximated by

$$\left[1+\frac{\Delta\tau}{2}\left(\frac{\partial\tilde{R}}{\partial t}\right)_n-\frac{\Delta\tau}{2}N\left(\frac{\partial^2}{\partial X^2}\right)\right]\Delta\varphi=\Delta\tau\left[N\left(\frac{\partial^2 t}{\partial X^2}+\frac{\partial^2 t}{\partial Y^2}\right)_n-\tilde{R}_n\right] \quad (18a)$$

$$\left(1-\frac{\Delta\tau}{2}N\frac{\partial^2}{\partial Y^2}\right)\Delta t=\Delta\varphi. \quad (18b)$$

To move ahead one time increment, equation (18a) is solved for $\Delta\varphi$. This is done by solving along grid points in the X direction for constant Y values. The $\Delta\varphi$ are then used on the right-side of equation (18b) which is solved for Δt along grid points in the Y direction for constant X values.

The rectangle has a grid as shown in Fig. 1(b). There are I and J points in the X and Y directions so the index ranges are, $1\leqslant i\leqslant I$ and $1\leqslant j\leqslant J$. Since all terms in equation (18) are at the time interval corresponding to the index n, this subscript will be omitted; the i, j subscripts are used to specify the X, Y location. Thus, the relations in equation (18) are for obtaining $\Delta t_{i,j}$ at all grid locations at time τ_n. This gives the temperatures for all X, Y at the new time by using $t_{n+1}=t_n+\Delta t_n$ at each grid point, i,j. Using equation (18a) a sweep is made in the X direction for each j to obtain the $\Delta\varphi_{i,j}$ for all i. Then using equation (18b) a sweep is made in the Y direction for each i to obtain $\Delta t_{i,j}$. To obtain the tridiagonal matrix for each sweep, variable increment sizes ΔX and ΔY are used within the region. The second derivatives are placed in finite difference form with ΔX^-, ΔX^+, ΔY^-, and ΔY^+ extending in the negative and positive coordinate directions as in Fig. 1(b)

$$\frac{\partial^2 t}{\partial X^2}=\frac{2t_{i+1,j}}{\Delta X^+(\Delta X^++\Delta X^-)}-\frac{2t_{i,j}}{\Delta X^+\Delta X^-}+\frac{2t_{i-1,j}}{\Delta X^-(\Delta X^++\Delta X^-)} \quad (19a)$$

$$\frac{\partial^2 t}{\partial Y^2}=\frac{2t_{i,j+1}}{\Delta Y^+(\Delta Y^++\Delta Y^-)}-\frac{2t_{i,j}}{\Delta Y^+\Delta Y^-}+\frac{2t_{i,j-1}}{\Delta Y^-(\Delta Y^++\Delta Y^-)} \quad (19b)$$

where $\Delta X^+=X_{i+1,j}-X_{i,j}$, and $\Delta X^-=X_{i,j}-X_{i-1,j}$, and similarly for ΔY.

Equation (19) is inserted into (18) with the result

$$-\frac{\Delta\tau N}{\Delta X^+(\Delta X^++\Delta X^-)}\Delta\varphi_{i+1,j}+\left(1+\frac{\Delta\tau}{2}\frac{\partial\tilde{R}_{i,j}}{\partial t}+\frac{\Delta\tau N}{\Delta X^+\Delta X^-}\right)\Delta\varphi_{i,j}-\frac{\Delta\tau N}{\Delta X^-(\Delta X^++\Delta X^-)}\Delta\varphi_{i-1,j}=\Delta\tau\left(\frac{2N}{\Delta X^++\Delta X^-}\left[\frac{t_{i+1,j}}{\Delta X^+}-\left(\frac{\Delta X^++\Delta X^-}{\Delta X^+\Delta X^-}\right)t_{i,j}+\frac{t_{i-1,j}}{\Delta X^-}\right]+\frac{2N}{\Delta Y^++\Delta Y^-}\left[\frac{t_{i,j+1}}{\Delta Y^+}-\left(\frac{\Delta Y^++\Delta Y^-}{\Delta Y^+\Delta Y^-}\right)t_{i,j}+\frac{t_{i,j-1}}{\Delta Y^-}\right]-\tilde{R}_{i,j}\right) \quad (20a)$$

$$\Delta t_{i,j} - \frac{\Delta\tau N}{\Delta Y^+ + \Delta Y^-}\left[\frac{\Delta t_{i,j+1}}{\Delta Y^+} - \left(\frac{\Delta Y^+ + \Delta Y^-}{\Delta Y^+ \Delta Y^-}\right)\Delta t_{i,j} + \frac{\Delta t_{i,j-1}}{\Delta Y^-}\right] = \Delta\varphi_{i,j}. \quad (20b)$$

Equations (20a) and (20b) are valid for all interior points $2 \leqslant i \leqslant I-1$, $2 \leqslant j \leqslant J-1$. At each boundary there is a zero normal temperature derivative as explained earlier. Hence equations (20) have special forms at the boundaries obtained by letting the temperature at a mirror image grid point outside the boundary be the same as at the first interior grid point value away from the boundary. Thus, for example, at $i = 1$, $j \neq 1, J$, equation (20a) is modified by letting the value at a fictitious point $i = 0$, $j \neq 1, J$ be $\varphi_{0,j} = \varphi_{2,j}$, and by letting $\Delta X^- = \Delta X^+$. This yields at $i = 1$, $j \neq 1, J$

$$\left[1 + \frac{\Delta\tau}{2}\left(\frac{\partial\tilde{R}_{1,j}}{\partial t}\right) + \frac{\Delta\tau N}{(\Delta X^+)^2}\right]\Delta\varphi_{1,j} - \frac{\Delta\tau N}{(\Delta X^+)^2}\Delta\varphi_{2,j} = \Delta\tau\left\{\frac{2N}{(\Delta X^+)^2}(t_{2,j} - t_{1,j}) + \frac{2N}{\Delta Y^+ + \Delta Y^-} + \left[\frac{t_{1,j+1}}{\Delta Y^+}\left(\frac{\Delta Y^+ + \Delta Y^-}{\Delta Y^+ \Delta Y^-}\right)t_{1,j} + \frac{t_{1,j-1}}{\Delta Y^-}\right] - \tilde{R}_{1,j}\right\}. \quad (21)$$

Equations (20a) and (20b) and the boundary condition relations as illustrated by equation (21) are assembled into the two tridiagonal matrices in the Appendix. Since $\tilde{R}(t)$ represents the radiation terms in equation (1), the $\partial\tilde{R}/\partial t$ needed for the b coefficients is

$$\frac{\partial\tilde{R}}{\partial t} = 4B_0\left[t^3(X, Y, \tau) - \frac{B_0}{4}\int_{X'=0}^{A_R}\int_{Y'=0}^{1} t^3(X', Y', \tau) \times \frac{S_1(B_0 R)}{R(X, Y, X', Y')}\,dX'\,dY'\right]. \quad (22)$$

The tridiagonal matrices are each solved using the well-known algorithm in refs. [24, 26]. The matrix (A1) gives a sweep of values across the X direction for each value of Y. Then the resulting $\Delta\varphi_{i,j}$ are used in matrix (A2) to obtain $\Delta t_{i,j}$ by making a sweep in the Y direction for each X. These Δt, which are at each X, Y are added to the $t(X, Y)$ to advance to the next time increment.

To evaluate the radiative source term $\tilde{R}(t)$ and $\partial\tilde{R}/\partial t$, that are in the matrix coefficients, an accurate integration method is required. The $S_1(B_0 R)$ is well behaved as $R \to 0$, but the $1/R$ factor makes the integrands of equations (1) and (22) appear to be singular as the integration variables X', Y' approach the grid point X, Y. The integrands are not singular as is evident by using cylindrical coordinates R, θ about X, Y. The $dX\,dY$ becomes $R\,dR\,d\theta$ and the $1/R$ is removed. However, when using rectangular coordinates for the purposes of integration, as in the present method, the apparent singularity must be considered for small R. For this reason, the integration surrounding each X, Y was divided into seven regions, Fig. 2(a). Region 7 is a small square of width less than one-half the local grid spacing. This was replaced by a small circle having the same area as the square, and the integration over region 7 carried out in cylindrical coordinates. This region provided only a small part of the total double integral, so this approximation did not yield significant error.

To carry out the integrations, the cross-section was covered with a grid of unevenly spaced points with more points near the boundaries where the temperature profiles have the largest curvature. For the integrations at each τ, two-dimensional spline fits were made of $t^4(X, Y, \tau)$ and $t^3(X, Y, \tau)$, as needed for $\tilde{R}(t)$ and $\partial\tilde{R}/\partial t$, using IMSL routines BSNAK and BS2IN. The spline coefficients were used to interpolate values at locations between grid points as called for by a two-dimensional integration subroutine. A Gaussian routine, SQUAD1 was used as described in ref. [27]. This uses 16 Gaussian points in each coordinate direction and was found in an earlier study [20] to provide excellent agreement with an IMSL Gaussian routine using more integration points and requiring significantly more computing time. By trying various numbers and sizes of the spatial increments, it was found that 19 unevenly spaced grid points across each direction (illustrated in Fig. 1(b)) gave accurate results for a square region. The increment size was small adjacent to the boundaries where four points spaced

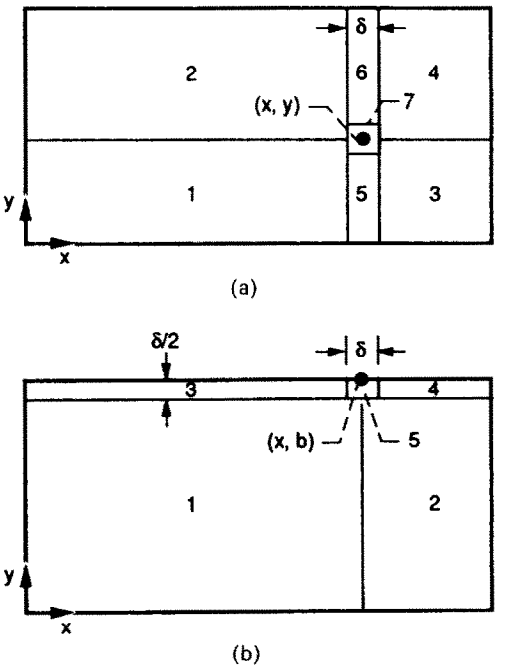

FIG. 2. Integration regions for evaluating local radiative source and local fluxes along boundary. (a) Regions for double integration for radiative source. (b) Regions for double integration for boundary flux.

0.02 apart were used. In the central portion of the region a spacing of 0.1 was found adequate. A similar spatial integration procedure with five subregions was used to determine the local heat fluxes along the boundary, Fig. 2(b).

To evaluate equation (3), $S_2(B_0R)$ values are required, and similarly $S_1(B_0R)$ values are needed for $\tilde{R}(t)$ defined in equation (13), and for $\partial\tilde{R}/\partial t$ in equation (22). The S_1 and S_2 functions were evaluated from equation (2) by using IMSL integration routine QAND, and function tables were prepared. Values of S_1 and S_2 for use in the two-dimensional integration routine were interpolated from the tables using IMSL cubic spline routines CSINT and CSVAL.

The calculations were carried out with a CRAY X-MP computer and required about 1 min per time increment for a 19 point grid (361 points in the square region). A variable time increment was used with the $\Delta\tau = 0.01$ initially, and then gradually increased through the calculation as the rate of temperature change decreased. The time increments were such that t_m changed about 0.02 for each time increment after using a few smaller increments at the beginning of the transient. About 20 time increments were used to reach a condition where about 40% of the initial energy in the region had been dissipated.

RESULTS AND DISCUSSION

Transient temperature distributions

Using the numerical solution procedure, transient temperature distributions were obtained in a square region. Typical results are in Fig. 3 for optical side lengths, $B_0 = 2$, 5, and 10, and for the conduction parameter $N = 0$, 0.1, and ∞. Because of symmetry, values are given along only one-half of a side or centerline. Parts (a)–(c) give values along the outer boundary, and part (d) along the centerline. When the transient begins, the hot region is suddenly subjected to a cold black environment and the outer portions of the region begin to cool the most rapidly. For finite heat conduction ($N > 0$) the conditions of the problem yield a zero temperature gradient normal to the boundaries. When B_0 is fairly small as in Fig. 3(a), the transient profiles are rather flat as is characteristic of an optically thin region. When the optical dimension is increased to 10, Fig. 3(c), the temperature distribution can be quite curved near the boundary as N approaches zero. For $N = 0.1$ the heat conduction is large enough to provide significant equalization of the temperature distribution across the region. There is less equalization early in the transient where the temperature distributions have been influenced more by the rapid action of the radiative transfer than by the slower action of energy diffusion by heat conduction.

The dimensionless temperature distribution is initially unity. Profiles are shown at four time values during the transient, corresponding to when approximately 3, 10, 25, and 40% of the initial energy in the region has been radiated away. For $N = 0.1$ the boundary temperatures in Fig. 3(a) are above those for $N = 0$. Conduction has somewhat equalized the temperatures over the cross-section thus raising the temperatures near the boundaries above those for zero conduction. When B_0 is increased to 10, Fig. 3(c), the transient surface temperature distributions without conduction are more curved, and heat conduction can then provide a more significant effect in raising the surface temperatures. This effect of N is shown more clearly by Fig. 3(d) which shows the temperature distribution along the centerline of the cross-section for $B_0 = 10$. Heat conduction results in increased temperatures at the boundary and decreased temperatures in the central region. For $B_0 = 10$ the central region cools much more slowly than the portions adjacent to the boundary

Transient surface heat fluxes

Figure 4 gives the local heat fluxes leaving through the boundary of a square region at the same times as in Fig. 3. The heat flux profiles become more curved as conduction decreases and the optical dimension of the region increases. As time advances, the decrease in temperature throughout the region reduces the radiative transfer, and the heat flux profiles become more flat. For $B_0 = 2$ the temperature distribution is already fairly flat when conduction is absent. Hence, the addition of conduction has little effect on the temperature profiles, and the resulting heat fluxes in Fig. 4(a) are practically independent of N. Figure 4(b), for $B_0 = 5$, shows a somewhat larger effect of N on the heat fluxes and the effect increases as the transient proceeds. For $B_0 = 10$, Fig. 4(c), heat conduction has a significant effect on the local radiated fluxes; results for $N = 0.3$ are also included. As the transient proceeds and the temperature level decreases, thereby reducing the relative importance of radiation, the curves for $N = 0.3$ gradually approach those for $N \to \infty$. Since the temperature distribution is uniform at the initiation of the transient, the numerical results for the initial surface fluxes were compared with the analytical solution in ref. [22], the values agreed to within a few tenths of 1 percent.

Transient mean temperature of square region

With regard to the total amount of energy that has been radiated away, the transient mean temperature of the region, $t_m(\tau)$ is of interest. This is shown in Fig. 5 for various B_0 and N. The ordinate is the ratio of $t_m(\tau)$ to the mean temperature that would be reached at the same time if the square region always had $t(X, Y, \tau)$ independent of X, Y and hence had the maximum emittance that could exist for the B_0 of the region (see equations (9) and (11)). The ratio is unity for $N \to \infty$ since the temperature distribution is uniform in this instance. For any finite N the rate of heat loss is smaller than for $N \to \infty$ so at any τ the $t_m(\tau)$ is larger than $t_{m,ut}(\tau)$; hence, the ratios in Fig. 5 are larger than unity. For design purposes the mean temperature $t_m(\tau)$ for various B_0 and N can be estimated

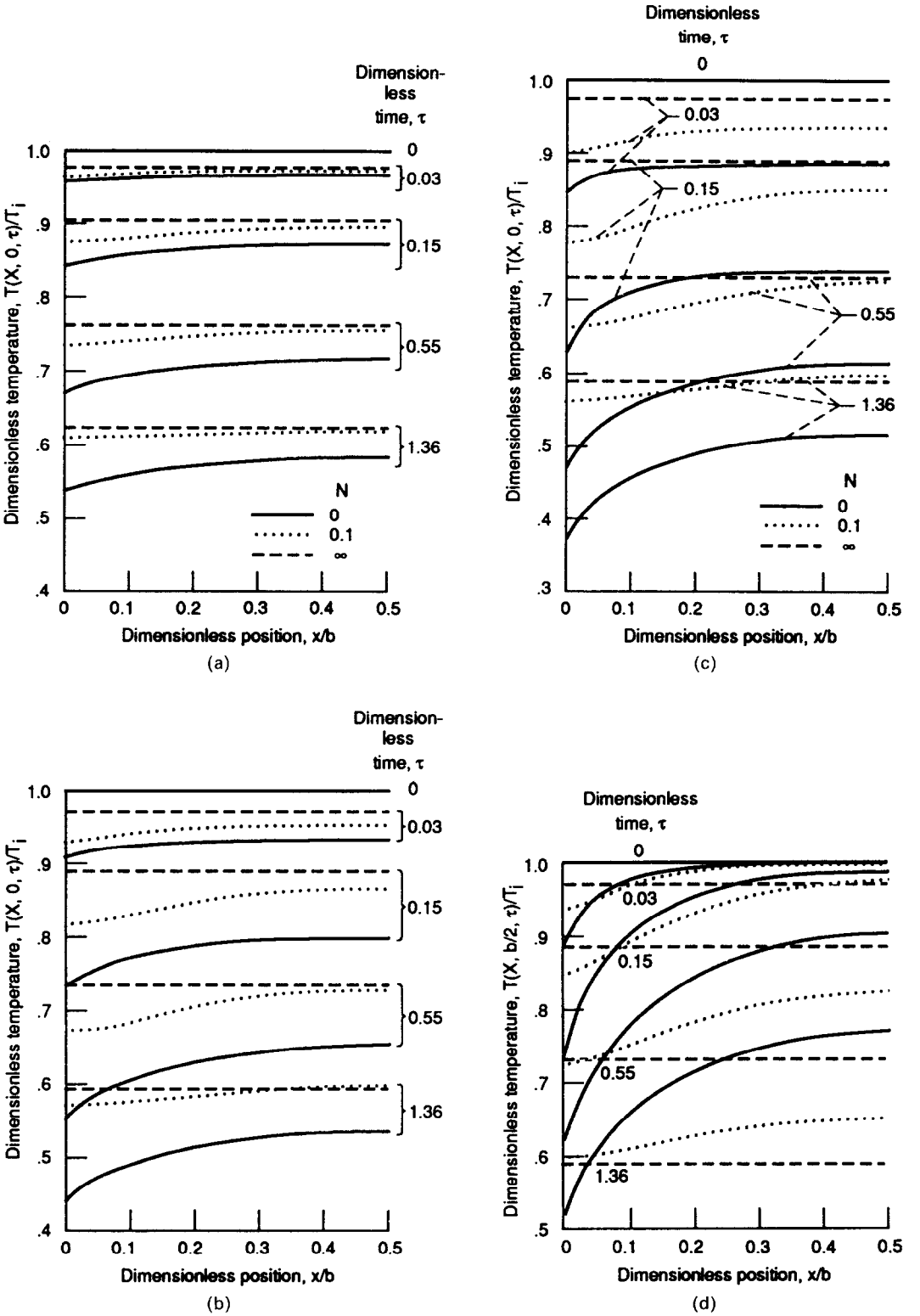

FIG. 3. Effect of heat conduction on transient temperature distributions for three optical side lengths. (a) Boundary temperatures, optical thickness, $B_0 = ab = 2$. (b) Boundary temperatures, optical thickness, $B_0 = ab = 5$. (c) Boundary temperatures, optical thickness, $B_0 = ab = 10$. (d) Centerline temperature distributions, $B_0 = ab = 10$.

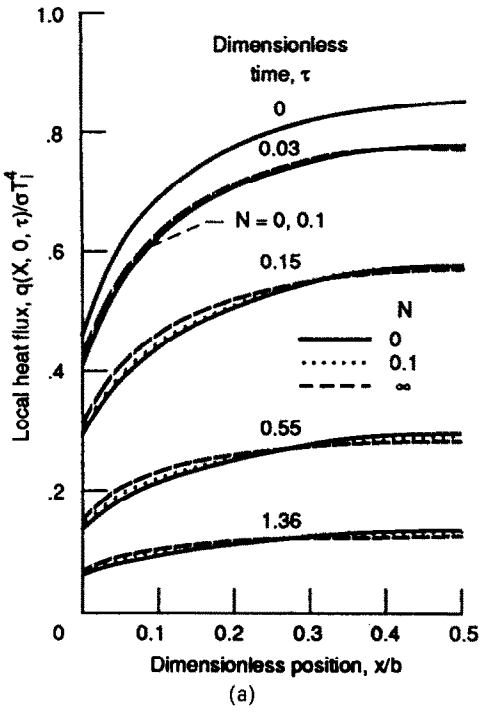

(a)

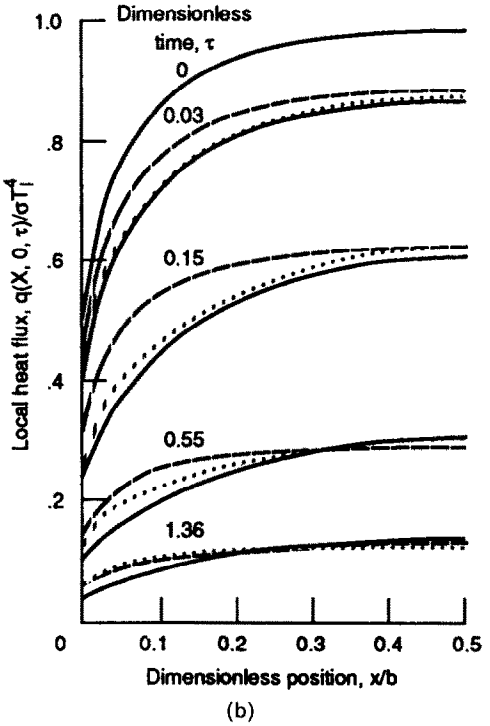

(b)

FIG. 4. Effect of heat conduction on transient boundary heat flux distributions for three optical side lengths. (a) Optical thickness, $B_0 = ab = 2$. (b) Optical thickness, $B_0 = ab = 5$. (c) Optical thickness, $B_0 = ab = 10$.

by using the ratios on the curves in conjunction with equation (11). For a small optical thickness the region always has a fairly uniform temperature distribution. It follows that for $B_0 = 2$, Fig. 5(a), the transient mean temperatures are only a few percent above the uniform temperature values. Consequently for

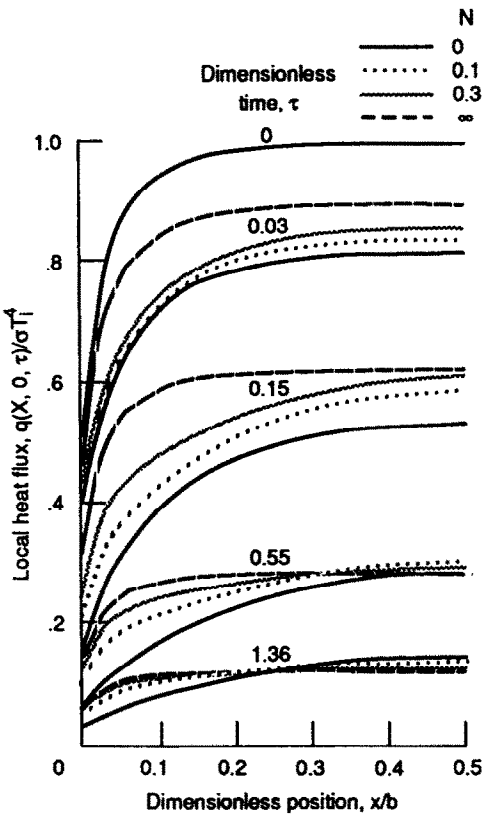

(c)

FIG. 4.—*Continued.*

$B_0 < 2$, the simple equation (9) can be used for any N to obtain very good results for the transient mean temperature. The ε_{ut} values for equation (9) can be obtained from the solution in ref. [22]. Some values are in Table 1, and a curve is in Fig. 6. When $N = 0.1$, Fig. 5(a) shows that agreement is obtained with equation (9) within less than 2% error when B_0 is 5 or less. Similarly from Fig. 5(b), for $N = 0.3$ agreement with equation (9) within 2% is obtained for B_0 as large as 10.

Transient overall heat loss from region

The instantaneous overall heat loss from the region is in Figs. 7(a) and (b). This is given as a ratio to the heat loss for a region with spatially uniform, but time varying, temperature, equation (12). Since $Q_{ut}(\tau)$ is easily calculated from equation (10) using available ε_{ut} values, the $Q(\tau)$ can be readily obtained for design purposes from the ratios given. During the early portion of the transient the rate of energy loss is lower than for a region with $t(X, Y, \tau)$ independent of X, Y. As time proceeds the ratios may become a little larger than unity. This is because the mean temperature has decreased more slowly than for the spatially uniform temperature case. As a result, late in the transient the mean temperature is large enough so that the heat loss may exceed that reached for the spatially uniform temperature case. For $B_0 < 2$ and any N, the transient

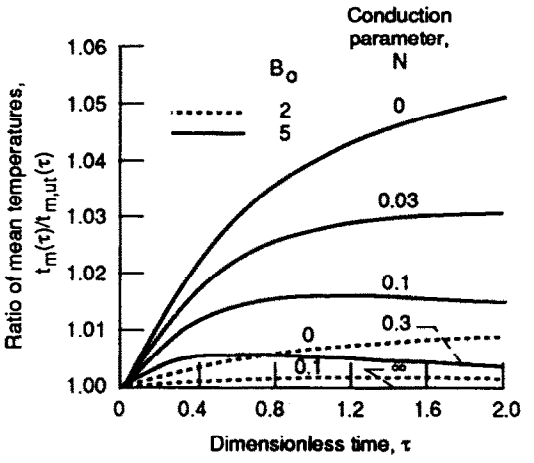

FIG. 5. Mean temperature of layer during transient cooling as compared with that for a layer cooling with uniform instantaneous temperature distribution. (a) Optical thickness, $B_0 = ab = 2$ and 5. (b) Optical thickness, $B_0 = ab = 10$.

Table 1. Overall emittance, $\varepsilon_{m,ut} = Q/4b\sigma T_m^4$, for a square region at uniform temperature

Optical length of side, B_0	$\varepsilon_{m,ut}$	Optical length of side, B_0	$\varepsilon_{m,ut}$
0.2	0.175	4	0.891
0.5	0.367	5	0.914
1	0.571	7	0.939
2	0.768	10	0.958
3	0.850	15	0.972

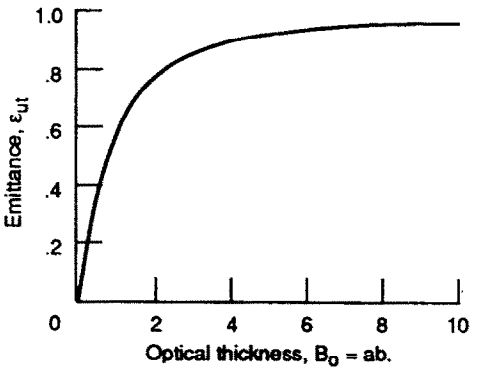

FIG. 6. Emittance for square region at uniform temperature.

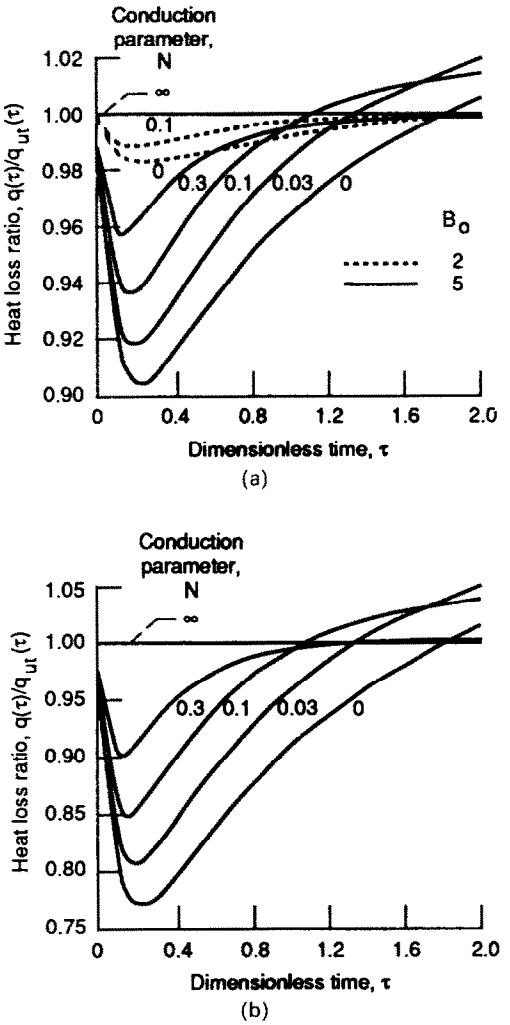

FIG. 7. Transient heat loss as compared with that for cooling with a uniform instantaneous temperature distribution. (a) Optical thickness, $B_0 = ab = 2$ and 5. (b) Optical thickness, $B_0 = ab = 10$.

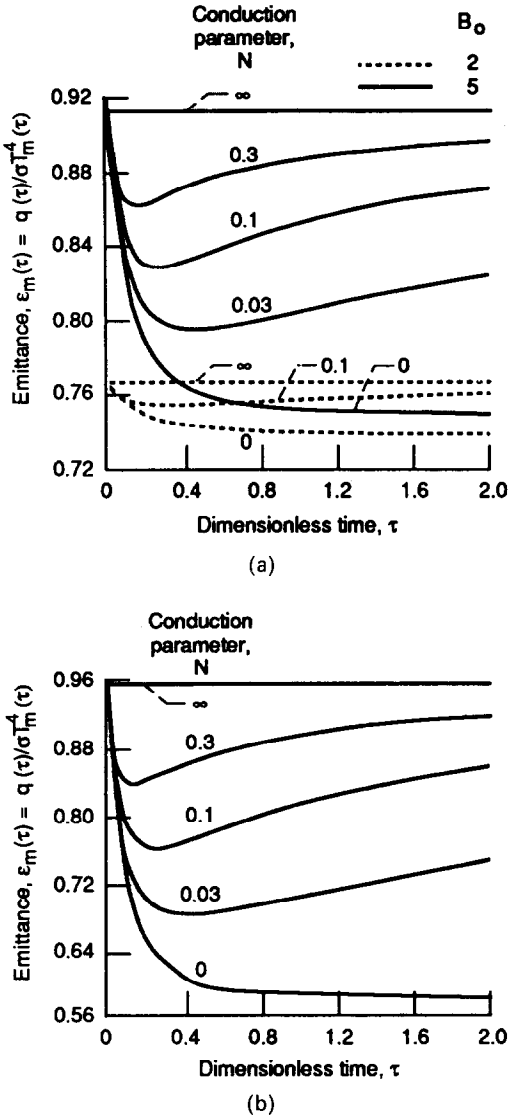

FIG. 8. Effect of conduction parameter and optical thickness on transient emittance. (a) Optical thickness, $B_0 = ab = 2$ and 5. (b) Optical thickness, $B_0 = ab = 10$.

heat loss differs by less than 2% from the values computed using a spatially uniform temperature distribution.

Transient emittance of region

From the transient mean temperature of the region, a transient emittance is calculated from equations (4) and (6). Results for $B_0 = 2$, 5, and 10 and various N values are in Fig. 8. $N = 0$ (radiation only) provides the largest transient emittance variation. For $N \to \infty$ the temperature distribution is uniform so $\varepsilon_m(\tau)$ remains at ε_{ut} throughout the transient. Since the region is initially at uniform temperature, the curves in Figs. 8(a) and (b) start at the ε_{ut} values. During the transient, the more pronounced cooling of the outer regions of the medium causes the instantaneous radiative loss to be smaller than that characteristic of the instantaneous mean temperature. As shown by the similarity solution in ref. [21], for no heat conduction the transient emittance decreases with time to a steady value that depends on B_0. With conduction, the temperature distribution gradually becomes more uniform as the transient proceeds. The transient emittance then increases toward its initial value corresponding to a uniform temperature region. This is an asymptotic approach, but the behavior is evident from the results shown.

CONCLUDING REMARKS

A solution procedure was developed for the transient cooling of a rectangular emitting, absorbing and heat conducting medium. Transient results were evaluated for a square region initially at uniform temperature, and then cooled by sudden exposure to a cold vacuum environment. Because of the boundary conditions, and the large variations in temperature that occur near the boundaries for some conditions, approximate methods based on diffusion or moment expansion methods are of questionable accuracy. It is demonstrated that direct numerical techniques can be applied without difficulty. A combination was used, of Gaussian integration and a finite difference method with variable spatial and time increments. Computer times on a CRAY X-MP were about 1 min for each time increment, and about 20 increments were required for a complete transient solution. Results for the transient mean temperature and overall heat loss of the region were compared with simple analytical expressions for a region always having a spatially uniform temperature during the cooling transient. The ranges of optical size and conduction parameter are shown within which this simple method will provide mean temperature and overall heat loss results accurate to within a few percent. Details are given for transient local surface heat fluxes for three optical dimensions of the region. The numerical method can be used to provide accurate detailed transient temperature distributions in a radiating and conducting medium.

REFERENCES

1. R. Siegel and J. R. Howell, *Thermal Radiation Heat Transfer*, 2nd Edn. Hemisphere, Washington, DC (1981).
2. P. S. Bathla and R. Viskanta, Effect of surroundings on the transient energy transfer in a layer of radiating gas, *Appl. Sci. Res.* **19**, 182–197 (1968).
3. R. Viskanta and P. S. Bathla, Unsteady energy transfer in a layer of gray gas by thermal radiation, *Z. Angew. Math. Phys. (ZAMP)* **18**, 353–367 (1967).
4. K. C. Weston and J. L. Hauth, Unsteady, combined radiation and conduction in an absorbing, scattering, and emitting medium, *J. Heat Transfer* **95**, 357–364 (1973).
5. T. H. Ping and M. Lallemand, Transient radiative–conductive heat transfer in flat glasses submitted to tem-

perature, flux and mixed boundary conditions, *Int. J. Heat Mass Transfer* **32,** 795–810 (1989).
6. C. C. Lii and M. N. Ozisik, Transient radiation and conduction in an absorbing, emitting, scattering slab with reflective boundaries, *Int. J. Heat Mass Transfer* **15,** 1175–1179 (1972).
7. C.-F. Tsai and G. Nixon, Transient temperature distribution of a multilayer composite wall with effects of internal thermal radiation and conduction, *Numer. Heat Transfer* **10,** 95–101 (1986).
8. R. Siegel, Transient radiative cooling of a droplet-filled layer, *J. Heat Transfer* **109,** 159–164 (1987).
9. B. Song and R. Viskanta, Deicing of solids using radiative heating, *J. Thermophys. Heat Transfer* **4,** 311–317 (1990).
10. R. Siegel, Finite difference solution for transient cooling of a radiating–conducting semitransparent layer, *J. Thermophys. Heat Transfer* **6,** 77–83 (1992).
11. W. A. Fiveland, Discrete-ordinates solutions of the radiative transport equation for rectangular enclosures, *J. Heat Transfer* **106,** 699–706 (1984).
12. J. S. Truelove, Discrete-ordinate solutions of the radiative transport equation, *J. Heat Transfer* **109,** 1048–1051 (1987).
13. M. M. Razzaque, D. E. Klein and J. R. Howell, Finite element solution of radiative heat transfer in a two-dimensional rectangular enclosure with gray participating media, *J. Heat Transfer* **105,** 933–936 (1983).
14. M. M. Razzaque, J. R. Howell and D. E. Klein, Coupled radiative and conductive heat transfer in a two-dimensional rectangular enclosure with gray participating media using finite elements, *J. Heat Transfer* **106,** 613–619 (1984).
15. W. W. Yuen and L. W. Wong, Analysis of radiative equilibrium in a rectangular enclosure with gray medium, *J. Heat Transfer* **106,** 433–440 (1984).
16. W. W. Yuen and C. F. Ho, Analysis of two-dimensional radiative heat transfer in a gray medium with internal heat generation, *Int. J. Heat Mass Transfer* **28,** 17–23 (1985).
17. W. W. Yuen and E. E. Takara, Analysis of combined conductive–radiative heat transfer in a two-dimensional rectangular enclosure with a gray medium, *J. Heat Transfer* **110,** 468–474 (1988).
18. C. F. Ho and M. N. Ozisik, Combined conduction and radiation in a two-dimensional rectangular enclosure, *Numer. Heat Transfer* **13,** 229–239 (1988).
19. W. W. Yuen and E. E. Takara, Superposition technique for radiative equilibrium in rectangular enclosures with complex boundary conditions, *Int. J. Heat Mass Transfer* **33,** 901–915 (1990).
20. R. Siegel, Transient cooling of a square region of radiating medium, *J. Thermophys. Heat Transfer* **5,** 495–501 (1991).
21. R. Siegel, Some aspects of transient cooling of a radiating rectangular medium, *Int. J. Heat Mass Transfer* **32,** 1955–1966 (1989).
22. R. Siegel, Analytical solution for boundary heat fluxes from a radiating rectangular medium, *J. Heat Transfer* **113,** 258–261 (1991).
23. W. W. Yuen and L. W. Wong, Numerical computation of an important integral function in two-dimensional radiative transfer, *J. Quant. Spectrosc. Radiat. Transfer* **29,** 145–149 (1983).
24. W. H. Press, B. P. Flannery, S. A. Teukolsky and W. T. Vetterling, *Numerical Recipes*. Cambridge University Press, New York (1989).
25. R. F. Warming and R. M. Beam, On the construction and application of implicit factored schemes for conservation laws. In *Computational Fluid Dynamics* (Edited by H. B. Keller), pp. 85–129. American Mathematical Society, Providence, Rhode Island (1978).
26. R. S. Varga, *Matrix Iterative Analysis*. Prentice-Hall, Englewood Cliffs, New Jersey (1962).
27. C. M. Goldstein, Numerical integration by Gaussian quadrature, NASA TM X-52088 (1965).

APPENDIX

The tridiagonal matrix to sweep in the X direction for each Y to determine the $\Delta\varphi_{i,j}$ is as follows:

$$\begin{bmatrix} b_{1,j} & c_{1,j} & & & & \\ a_{2,j} & b_{2,j} & c_{2,j} & & & \\ & a_{3,j} & b_{3,j} & c_{3,j} & & \\ & & \cdot & \cdot & \cdot & \\ & & & \cdot & \cdot & c_{I-1,j} \\ & & & & a_{I,j} & b_{I,j} \end{bmatrix} \begin{bmatrix} \Delta\varphi_{1,j} \\ \Delta\varphi_{2,j} \\ \Delta\varphi_{3,j} \\ \cdot \\ \cdot \\ \Delta\varphi_{I,j} \end{bmatrix} = \begin{bmatrix} S_{1,j} \\ S_{2,j} \\ S_{3,j} \\ \cdot \\ \cdot \\ S_{I,j} \end{bmatrix}, \tag{A1}$$

where the terms are

For $1 \leqslant j \leqslant J$

$$a_{i,j} = -\frac{N\Delta\tau}{\Delta X^-(\Delta X^+ + \Delta X^-)} \quad 2 \leqslant i \leqslant I-1; \quad a_{I,j} = -\frac{N\Delta\tau}{(\Delta X^-)^2}$$

$$b_{1,j} = 1 + \frac{\Delta\tau}{2}\frac{\partial \tilde{R}_{1,j}}{\partial t} + \frac{N\Delta\tau}{(\Delta X^+)^2}$$

$$b_{i,j} = 1 + \frac{\Delta\tau}{2}\frac{\partial \tilde{R}_{i,j}}{\partial t} + \frac{N\Delta\tau}{\Delta X^+ \Delta X^-} \quad 2 \leqslant i \leqslant I-1$$

$$b_{I,j} = 1 + \frac{\Delta\tau}{2}\frac{\partial \tilde{R}_{I,j}}{\partial t} + \frac{N\Delta\tau}{(\Delta X^-)^2}$$

$$c_{1,j} = -\frac{N\Delta\tau}{(\Delta X^+)^2}; \quad c_{i,j} = -\frac{N\Delta\tau}{\Delta X^+(\Delta X^+ + \Delta X^-)} \quad 2 \leqslant i \leqslant I-1.$$

For $2 \leqslant j \leqslant J-1$

$$S_{1,j} = \Delta\tau\left\{\frac{2N}{(\Delta X^+)^2}(t_{2,j}-t_{1,j}) - \tilde{R}_{1,j} + 2N\left[\frac{t_{1,j+1}}{\Delta Y^+(\Delta Y^+ + \Delta Y^-)} - \frac{t_{1,j}}{\Delta Y^+ \Delta Y^-} + \frac{t_{1,j-1}}{\Delta Y^-(\Delta Y^+ + \Delta Y^-)}\right]\right\}$$

$$S_{i,j} = \Delta\tau\left\{2N\left(\frac{t_{i+1,j}}{\Delta X^+(\Delta X^+ + \Delta X^-)} - \frac{t_{i,j}}{\Delta X^+ \Delta X^-} + \frac{t_{i-1,j}}{\Delta X^-(\Delta X^+ + \Delta X^-)}\right) - \tilde{R}_{i,j} + 2N\left[\frac{t_{i,j+1}}{\Delta Y^+(\Delta Y^+ + \Delta Y^-)} - \frac{t_{i,j}}{\Delta Y^+ \Delta Y^-} + \frac{t_{i,j-1}}{\Delta Y^-(\Delta Y^+ + \Delta Y^-)}\right]\right\}$$

$$S_{I,j} = \Delta\tau\left\{\frac{2N}{(\Delta X^-)^2}(t_{I-1,j}-t_{I,j}) - \tilde{R}_{I,j} + 2N\left[\frac{t_{I,j+1}}{\Delta Y^+(\Delta Y^+ + \Delta Y^-)} - \frac{t_{I,j}}{\Delta Y^+ \Delta Y^-} + \frac{t_{I,j-1}}{\Delta Y^-(\Delta Y^+ + \Delta Y^-)}\right]\right\}$$

$$\Delta X^+ = X_{i+1,j} - X_{i,j} \qquad \Delta Y^+ = Y_{i,j+1} - Y_{i,j}$$

$$\Delta X^- = X_{i,j} - X_{i-1,j} \qquad \Delta Y^- = Y_{i,j} - Y_{i,j-1}.$$

If $j = 1$ replace [ ] by $\dfrac{1}{(\Delta Y^+)^2}(t_{i,2}-t_{i,1}) \quad 1 \leqslant i \leqslant I.$

If $j = J$ replace [ ] by $\dfrac{1}{(\Delta Y^-)^2}(t_{i,J-1}-t_{i,J}) \quad 1 \leqslant i \leqslant I.$

The tridiagonal matrix to sweep in the Y direction for each X to determine the $\Delta t_{i,j}$ is

$$\begin{bmatrix} B_{i,1} & C_{i,1} & & & & \\ A_{i,2} & B_{i,2} & C_{i,2} & & & \\ & \cdot & \cdot & \cdot & & \\ & & \cdot & \cdot & \cdot & \\ & & & \cdot & \cdot & C_{i,J-1} \\ & & & & A_{i,J} & B_{i,J} \end{bmatrix} \begin{bmatrix} \Delta t_{i,1} \\ \Delta t_{i,2} \\ \cdot \\ \cdot \\ \cdot \\ \Delta t_{i,J} \end{bmatrix} = \begin{bmatrix} \Delta\varphi_{i,1} \\ \Delta\varphi_{i,2} \\ \cdot \\ \cdot \\ \cdot \\ \Delta\varphi_{i,J} \end{bmatrix} \tag{A2}$$

where the coefficients are

$$A_{i,j} = -\frac{N\Delta\tau}{\Delta Y^-(\Delta Y^+ + \Delta Y^-)} \quad 2 \leqslant j \leqslant J-1; \quad A_{i,J} = -\frac{N\Delta\tau}{(\Delta Y^-)^2}$$

$$B_{i,1} = 1 + \frac{N\Delta\tau}{(\Delta Y^+)^2}; \quad B_{i,J} = 1 + \frac{N\Delta\tau}{(\Delta Y^-)^2}$$

$$B_{i,j} = 1 + \frac{N\Delta\tau}{\Delta Y^+ \Delta Y^-} \quad 2 \leqslant j \leqslant J-1$$

$$C_{i,1} = -\frac{N\Delta\tau}{(\Delta Y^+)^2}; \quad C_{i,j} = -\frac{N\Delta\tau}{\Delta Y^+(\Delta Y^+ + \Delta Y^-)} \quad 2 \leqslant j \leqslant J-1.$$

SOLUTION DE DIFFERENCES FINIES POUR LE REFROIDISSEMENT RADIATIF VARIABLE D'UN DOMAINE CARRE CONDUCTEUR ET SEMI-TRANSPARENT

Résumé—On obtient les solutions transitoires pour un domaine carré de matériau conducteur semi-transparent refroidi par rayonnement thermique. Ce domaine est placé dans le vide et l'énergie est dispersée seulement par rayonnement à partir des limites du domaine. L'effet de la conduction est de répartir partiellement la distribution interne de température. Lorsque l'épaisseur optique du domaine augmente, les gradients de température croissent près des frontières et des coins, à moins que la conduction thermique soit grande. La procédure de résolution peut fournir des distributions de température précise dans ces régions pour éviter une erreur dans le calcul des pertes par rayonnement. Une intégration gaussienne numérique bidimensionnelle est utilisée pour obtenir le terme de source radiative locale. Une procédure aux différences finies avec incréments variables d'espace et de temps est utilisée pour résoudre l'équation d'énergie transitoire. Un espacement variable est utilisé pour concentrer les points de la grille dans les régions à grands gradients de température.

BERECHNUNG DER TRANSIENTEN STRAHLUNGSKÜHLUNG EINES WÄRMELEITENDEN HALBTRANSPARENTEN QUADRATISCHEN GEBIETS MITTELS FINITER DIFFERENZEN

Zusammenfassung—Die Strahlungskühlung eines quadratischen Gebiets aus wärmeleitendem halbstransparentem Material wurde für instationäre Bedingungen berechnet. Das Gebiet befindet sich in einer evakuierten Umgebung, so daß Energie ausschließlich durch Strahlung aus dem Medium durch seine Berandung hindurch transportiert werden kann. Die Wärmeleitung führt während des transienten Vorgangs zu einem teilweisen Ausgleich der Temperaturverteilung im Inneren. Trotz der starken Wärmeleitung werden die Temperaturgradienten mit wachsender optischer Dicke des Gebiets an dessen Begrenzungen und in Ecken größer. Das Lösungsverfahren muß in der Lage sein, genaue Temperaturverteilungen in diesen Gebieten zu liefern, um Fehler im berechneten Strahlungsverlust zu vermeiden. Die örtlichen Strahlungsquellterme wurden mit Hilfe einer zweidimensionalen numerischen Integration nach Gauss ermittelt. Die instationäre Energiegleichung wird mittels eines Finite-Differenzen-Verfahrens mit variabler Orts- und Zeitschrittweite gelöst. Die variable Schrittweite ist erforderlich, um in Bereichen mit starken Temperaturgradienten Knotenpunkte konzentrieren zu können.

РЕШЕНИЕ КОНЕЧНО-РАЗНОСТНЫМ МЕТОДОМ ЗАДАЧИ НЕСТАЦИОНАРНОГО ОХЛАЖДЕНИЯ ИЗЛУЧЕНИЕМ ТЕПЛОПРОВОДЯЩЕЙ ПОЛУПРОЗРАЧНОЙ КВАДРАТНОЙ ОБЛАСТИ

Аннотация—Получены нестационарные решения для охлаждения квадратной области теплопроводящего полупрозрачного материала за счет теплового излучения. Область находится в вакууме, поэтому энергия рассеивается только излучением. Эффект теплопроводности при нестационарном процессе способствует выравниванию внутреннего распределения температур. С ростом оптической толщины области температурные градиенты возле границ и углов увеличиваются, если теплопроводность невелика. Во избежание погрешностей в расчетах потерь на излучение методика решения должна обеспечивать точное определение распределений температур в исследуемых областях. Для нахождения локального источника излучения используется двумерное численное гауссовское интегрирование. Нестационарное уравнение сохранения энергии решается конечно-разностным методом с изменяющимися пространственными и временными шагами. С целью контентрации точек сетки в областях с большими температурными градиентами использовался переменный шаг.